Received: 12 April 2021 | Revised: 18 August 2021 | Accepted: 25 August 2021

DOI: 10.1111/faf.12613

FISH and FISHERIES WILEY

ORIGINAL ARTICLE

Contrasting climate velocity impacts in warm and cool locations show that effects of marine warming are worse in already warmer temperate waters

Philina A. English[1] | Eric J. Ward[2] | Christopher N. Rooper[1] | Robyn E. Forrest[1] | Luke A. Rogers[1] | Karen L. Hunter[1] | Andrew M. Edwards[1,3] | Brendan M. Connors[4] | Sean C. Anderson[1,5]

[1]Pacific Biological Station, Fisheries and Oceans Canada, Nanaimo, BC, Canada

[2]Northwest Fisheries Science Centre, National Marine Fisheries Service, National Oceanographic and Atmospheric Administration, Seattle, WA, USA

[3]Department of Biology, University of Victoria, Victoria, BC, Canada

[4]Institute of Ocean Sciences, Fisheries and Oceans Canada, Sidney, BC, Canada

[5]Department of Mathematics, Simon Fraser University, Burnaby, BC, Canada

Correspondence
Philina A. English, Pacific Biological Station, Fisheries and Oceans Canada, Nanaimo, BC, Canada.
Email: philina.english@dfo-mpo.gc.ca

Funding information
Fisheries and Oceans Canada, Grant/Award Number: Aquatic Climate Change Adaptation Services Program

Abstract

Species responses to climate change are often measured at broad spatiotemporal scales, which can miss the fine-scale changes that are most relevant to conservation and fisheries management. We develop a scaleable geostatistical approach to assess how juvenile and adult fish distributions have been shaped by changes in bottom temperature and dissolved oxygen over a recent decade of warming in the northeast Pacific. Across 38 demersal fishes, biomass trends were associated negatively with warming and positively with dissolved oxygen, but when trends in both biomass and climate were converted to velocities—the speed and direction a population would have to move to maintain consistent conditions—the effect of temperature change differed depending on local conditions. In the warmest locations, warming velocities were associated with negative biotic velocities for 19 of 69 species-maturity combinations, and yet were almost always associated with stable or positive biotic velocities in the coolest locations (64 of 69). These spatially consistent biomass declines (negative biotic velocities) in the warmest locations and increases in cooler locations suggest a redistribution of species with the potential for new ecological and fisheries interactions. After controlling for temperature, the more spatially consistent effects of dissolved oxygen were often negative, suggesting a mechanism other than hypoxia avoidance—potentially changes in primary production. Our approach identifies the species and locations that are most sensitive to observed changes in the environment at any scale, thus facilitating future vulnerability assessments.

KEYWORDS

biotic velocity, climate change, context dependence, dissolved oxygen, groundfish, spatiotemporal distribution models

1 | INTRODUCTION

Managing the impacts of a rapidly changing climate on ecological communities, particularly those that provide food for humans, is a critical challenge facing society (e.g. Doney et al., 2012). An increase in atmospheric CO_2 is not only causing increases in both mean ocean temperature and the frequency of extreme heat waves (Frölicher et al., 2018), but is also affecting patterns of circulation, productivity and marine chemistry (Pörtner et al., 2019). Combined, these environmental changes can impact the distribution and abundance of many ecologically and commercially important fish species, leading to local loss of some species, colonizations, and changes in species interactions and bycatch composition (e.g. García Molinos et al., 2016; Morley et al., 2018; Pinsky & Fogarty, 2012). Furthermore, such changes can cause the efficiency of fishing to increase if population density increases faster than range expansion during population growth, or temporarily maintain catch rates despite population decline if the organisms move towards preferred habitat as it becomes available (the basin model of density-dependent habitat selection theory; MacCall, 1990, Thorson et al., 2016). Because traditional stock assessment methods, fisheries regulations and choices regarding habitat protection generally assume stationary species distributions, new methods that anticipate and incorporate the effects of climate change on species distributions will be crucial for successful resource management in the future (Bell et al., 2020; Hare et al., 2010).

Species responses to climate change are often studied along range edges (Fredston et al., 2020; Fredston-Hermann et al., 2020; Parmesan & Yohe, 2003; Sunday et al., 2015) or as aggregate indices (e.g. at species or region levels; Morley et al., 2018; Pinsky et al., 2013; Thorson et al., 2016). The centre of gravity is perhaps the most commonly used measure of changes in distribution for marine fishes (e.g. Adams et al., 2018; Dulvy et al., 2008; Nye et al., 2009; Perry et al., 2005; Rindorf & Lewy, 2006; Rooper et al., 2020). However, these approaches can overlook fine-scale spatial variation that may be important for understanding species responses (Oldfather et al., 2020), and distribution shifts may take longer to manifest at aggregate scales. Aggregate measures such as the centre of gravity are also challenging to interpret and apply in cases where both surveys and management actions are constrained by geographic or political boundaries that partition the distribution of a species. Indeed, laboratory experiments have demonstrated that thermal tolerances and optimums can differ sub-regionally (e.g. Pörtner et al., 2008), and there is evidence that warm range edges have shifted farther north than expected and cold range edges contracted southward (in the northern hemisphere), which suggest roles for competition, predator-prey interactions and/or density-dependent habitat selection (Fredston et al., 2020). Despite this, projections of future species' distributions often assume that responses to climate variables are consistent across space and time (e.g. Morley et al., 2018). While coarse-scale changes can be informative for long-term planning, changes in local abundances at finer spatial scales will likely occur more quickly due to the shorter dispersal distances involved and may be more informative in steering local conservation actions.

Local velocities are commonly used to quantify changes at finer spatial scales than are captured in population-wide indices (e.g. centre of gravity; Brito-Morales et al., 2018). A local climate velocity represents the movement of an isocline—a boundary along which a climate metric is constant. More intuitively, a climate velocity gives the speed and direction a population must move to maintain a constant climate condition (Loarie et al., 2009). Gradient-based estimates of climate velocity are calculated as a trend in a climate metric through time (e.g. temperature trend), which can be positive or negative, divided by the local gradient in space comprised of a magnitude and direction (see Methods Equation 12; Table 1; Burrows et al., 2011). These velocities scale local climate trends to emphasize locations where climate is relatively consistent across a neighbourhood of cells. Alternatively, analogue-based velocities are estimated using search algorithms that identify nearest climate matches within a user-defined threshold of change from the reference cell conditions (Hamann et al., 2015). While analogue-based velocity estimates can be more geographically precise, the choice of thresholds and other statistical properties (e.g. clumpiness) make them less useful than gradient-based local velocities for meta-analysis (Ordonez & Williams, 2013).

Changes in abundance, density or probability of species occurrence can also be expressed as velocities (e.g. Alabia et al., 2018; Comte & Grenouillet, 2015; Serra-Diaz et al., 2014). When applied to species distribution models, these are referred to as biotic velocities and can be thought of as the minimum distance one would have to move to maintain an equivalent degree of habitat suitability (Carroll

TABLE 1 Gradient-based velocity metrics and their definitions. Climatic variables are temperature and dissolved oxygen (DO); biotic variables are biomass density for the mature and immature components of a species. Climatic and biotic variables are represented generically by *A*. Our analysis treated gradient-based velocity as a scalar, using only the magnitude component of the velocity vector

Term	Notation	Definition	Magnitude	Sign
Local trend	$m_s^A = \frac{\Delta A_s}{\Delta t}$	Change in local biotic or climatic scalar *A* per decade	Temporal rate of change in *A*	Increasing (+) or decreasing (−) local trend in *A*
Spatial gradient	$\overline{g}_s^A$	Vector sum (magnitude, angle) of mean north or south and east or west gradients of *A* in a 3 × 3 cell spatial neighbourhood	Spatial rate of change in *A*	Vector magnitude and angle always positive (+)
Gradient-based velocity	$\overline{V}_s^A = \frac{m_s^A}{\overline{g}_s^A}$	Vector velocity (magnitude, angle) from local trend of *A* divided by vector local spatial gradient of *A*	Speed of travel predicted to maintain initial *A*	Increasing (+) or decreasing (−) based on the local trend in *A*

et al., 2015; Comte & Grenouillet, 2015). Similar to climate velocity, a positive local biotic velocity is associated with an increase in habitat suitability at the focal location and a negative value represents a decline in suitability. The magnitude of the velocity estimates the distance to the nearest location that is predicted to match the original probability of occurrence or abundance after a given period of time. Because changes in climate may cause shifts in fish population density before range shifts based on presence-absence are clearly detectable, abundance and biomass-based models of species distributions are potentially more sensitive to local change than simple occupancy estimates.

Bottom-trawl fisheries tend to capture a taxonomically and ecologically diverse suite of fishes. For example, the groundfish bottom-trawl fishery in Canadian Pacific waters encounters >100 species (Anderson et al., 2019), many of which are managed via an individual transferable quota system with 100% at sea and dockside monitoring (DFO, 2019; Turris, 2000; Wallace et al., 2015). Random depth-stratified fishery-independent bottom-trawl surveys have been fitted with conductivity, temperature, depth (CTD) and dissolved oxygen (DO) sensors since 2008. In addition to estimates of biomass density for each species captured in the surveys, data on size distributions and reproductive maturity are collected for many species (Anderson et al., 2019). Collectively, these species occupy a large range of depths, especially along the shelf edge where short movements can result from large environmental changes, and vary in their potential for behavioural responses to climate. For example, some species are migratory or highly mobile (e.g. Sablefish (*Anoplopoma fimbria*, Anoplopomatidae) and many flatfish species (Pleuronectidae)), while others are relatively sedentary (e.g. many species of rockfish, *Sebastes* spp. (Sebastidae)). Furthermore, a warmer ocean is expected to hold less oxygen, while becoming more stratified (Levin & Le Bris, 2015), and groundfish species occupying different depths vary in their sensitivity to hypoxia (Keller et al., 2017).

Here, we explore the extent to which groundfish distributions in the northeast Pacific have been shaped by local temperature and DO trends and velocities over a decade spanning a relatively cool period through a recent marine heat wave (Frölicher & Laufkötter, 2018; Okey et al., 2014). We do this by quantifying broad patterns and species-level relationships between climatic and biotic change in order to answer the following questions: (a) Are local changes in bottom temperature or DO correlated with changes in local groundfish densities, and are these effects stronger in already warm or low-oxygen regions? For example, has local warming had a larger effect in locations that are already at the warm-extreme of a species' local distribution? (b) How do these relationships differ between the spatial contexts captured by gradient-based velocities versus their component trends? (c) How do these effects vary between species, and are they correlated with life-history characteristics such as age and growth rate or ecological traits such as depth range, latitude, trophic level, foraging zone, or sociality? We address these questions by using spatiotemporal models applied to a decade of survey-derived climate and species density data, and then assess relationships between velocities of biotic and climatic change for 38 commonly

encountered species using a geostatistically explicit hierarchical analysis that controls for change in both temperature and DO.

2 | METHODS

2.1 | Survey data

We analysed biomass density distributions and morphometric data for 38 species of groundfish that were regularly encountered by fisheries-independent bottom-trawl surveys and are widely distributed within Canadian Pacific waters (DFO, 2020, Table S1). The surveys were stratified within four regions (Figure 1a), two of which were surveyed in odd years (Hecate Strait and Queen Charlotte Sound) and two in even years (West Coast Vancouver Island and West Coast Haida Gwaii) since at least 2005. Each region was sampled over the same month long period between late May and early August in each survey year (Figure S1). These surveys shared similar random depth-stratified designs, fishing gear and fishing protocols (Sinclair et al., 2003). Combined, they covered most of the upper continental slope and shelf in Pacific Canada, and resulted in a mean of 326 samples per year (range from 200 to 436). We only included tows of >15 min duration and converted total biomass of each species to a biomass density based on the speed, distance covered, and net opening (e.g. Anderson et al., 2019; Williams et al., 2018). Biological sampling protocols varied among species, depending on size of catch and commercial importance. In general, catches of between 10–50 fish were sexed, weighed and measured individually, while larger catches were subsampled and, for commercially important species, maturity data and otoliths for ageing were collected.

2.2 | Estimating spatiotemporal variation in maturity-specific biomass density

Because ontogenetic shifts in habitat, particularly depth, are well documented for groundfish species (e.g. Barbeaux & Hollowed, 2018; Li et al., 2019; Mindel et al., 2016), we estimated biomass densities separately for mature and immature size classes whenever possible. Maturity was not assessed for certain Chondrichthyans, or when catches were particularly low. We first estimated length at 50% maturity as defined by gonadal development stages using ogives fit as sex-specific logistic regressions to individual specimens (see Methods S1). To split the estimated biomass density per tow into mature and immature components, we calculated the summed biomass of all measured fish that were above (for mature) or below (for immature) the length-at-50% maturity threshold, divided by the total biomass of all measured fish, and multiplied this ratio by the estimated biomass density for each tow. For each tow that resulted in too small a catch for detailed measurements to have been taken, we applied the mean ratio from all measured tows to estimate mature biomass (applied to a median of 9% (range 1%–40%) of each species' total sampled biomass). For species without any maturity data, we assumed that the total biomass estimate represented the mature population, because mature individuals are larger and therefore likely to be proportionally dominant (* in Table S1). However, it is possible that biomass sampled in some areas was actually dominated by immature individuals, particularly for the skate species, whose mean lengths fall close to the sizes at maturity found in Love (2011).

We modelled spatiotemporal biomass density separately for mature and immature fish of each species using spatial Generalized Linear Mixed Effects Models (GLMMs). Environmental variables, such as temperature, may be included in these models explicitly and can be used to assess the vulnerability or tolerance of a given species to change (Godefroid et al., 2019). However, such approaches require strong assumptions (e.g. that effects are constant through both time and space). Instead, we used a climate-agnostic version of a species distribution model with a spatiotemporal random effect structure to estimate local variability in biomass density change. Our models relied on spatial random effects to capture unmeasured components of habitat suitability and allow suitability to change through time without making assumptions about the shape of species-specific responses to possible climatic and geographic covariates (e.g. Shelton et al., 2014; Thorson et al., 2015, 2017; Ward et al., 2015). We modelled each species and maturity class separately because, although these density patterns are correlated, explicitly modelling those relationships among groundfish species has not been shown to dramatically improve precision of overall estimates (Thorson & Barnett, 2017), and maintaining independent estimates should make identification of shared climate responses more conservative.

We modelled biomass density with a Tweedie distribution and a log link because densities contain both zeros and positive continuous values (Anderson et al., 2019; Dunn & Smyth, 2005; Tweedie, 1984):

$$Y_{s,t} \sim \text{Tweedie}\left(\mu_{s,t}, p, \phi\right),\ 1 < p < 2, \tag{1}$$

$$\mu_{s,t} = \exp\left(\alpha_t + \gamma_{1,t} D_{s,t} + \gamma_{2,t} D_{s,t}^2 + \omega_s + \varepsilon_{s,t}\right), \tag{2}$$

$$\gamma_{1,t} \sim \text{Normal}\left(\gamma_{1,t-1}, \sigma_{\gamma_1}^2\right), \tag{3}$$

$$\gamma_{2,t} \sim \text{Normal}\left(\gamma_{2,t-1}, \sigma_{\gamma_2}^2\right), \tag{4}$$

$$\boldsymbol{\omega} \sim \text{MVNormal}\left(0, \boldsymbol{\Sigma}_{\omega}\right), \tag{5}$$

$$\boldsymbol{\varepsilon}_t \sim \text{MVNormal}\left(0, \boldsymbol{\Sigma}_{\varepsilon}\right), \tag{6}$$

where $Y_{s,t}$ represents the biomass density at point in space s and time t, μ represents the mean biomass density, p represents the Tweedie power parameter, and ϕ represents the Tweedie dispersion parameter. The parameter α_t represents the mean effect for each year, and $\gamma_{1,t}$ and $\gamma_{2,t}$ represent time-varying coefficients associated with depth (D) and depth-squared covariates (D^2), respectively, which both follow a random walk constrained by $\sigma_{\gamma_1}^2$ and $\sigma_{\gamma_2}^2$. The initial values $\gamma_{1,t}$ and $\gamma_{2,t}$

at $t = 1$ share an implied Uniform$(-\infty, \infty)$ prior. We considered alternative covariates not described here (see Methods S2). The parameters ω_s and $\varepsilon_{s,t}$ represent spatial and spatiotemporal random effects that were assumed drawn from Gaussian Markov random fields (e.g. Cressie & Wikle, 2011; Latimer et al., 2009; Lindgren et al., 2011) with covariance matrices $\mathbf{\Sigma}_\omega$ and $\mathbf{\Sigma}_\varepsilon$ that were constrained by Matérn covariance functions (Cressie & Wikle, 2011). The covariance matrices for a given maturity-species combination shared a common κ parameter that controls the rate of decay of spatial correlation with distance (Cressie & Wikle, 2011).

We modelled the spatial components as random fields using a triangulated mesh with vertices selected using a k-means algorithm (via the k-means function in R; e.g. Shelton et al., 2014) at a specified number of locations, known as knots, used to approximate the spatial variability in observations. We used 500 knots for mature density, 400 for immature density, and 300 for less well-sampled species (Boccaccio *Sebastes paucispinis*, Shortraker Rockfish *S. borealis*, and immature Redstripe Rockfish *S. proriger*). Based on estimated values of the spatial surface at these knot locations, we used bilinear interpolation to approximate a continuous spatial field (Lindgren et al., 2011; Rue et al., 2009).

We fit our models in R version 3.6.1 (R Core Team, 2019) with the R package `sdmTMB` (Anderson et al., 2019, 2020), which interfaces automatic differentiation and the Laplace approximation in the `TMB` (Template Model Builder) R package (Kristensen et al., 2016) with the SPDE (Stochastic Partial Differential Equation) approximation to Gaussian Markov fields from the `INLA` (Integrated Nested Laplace Approximation) R package (Rue et al., 2009) to find the value of the fixed effects that minimizes the marginal negative log likelihood. We confirmed that the non-linear optimizer had converged by checking that the Hessian matrix was positive definite and the maximum absolute gradient across fixed effects was <0.005.

2.3 | Climate trends and velocities

Bottom temperature and dissolved oxygen (DO) levels have been collected on most tows during the synoptic bottom-trawl surveys since 2008 using Seabird Electronics SBE 19 profilers. From these measurements, we predicted seafloor climate using an approach similar to the one described above for biomass density except that we used a Gaussian observation model, 800 knots, and allowed the spatiotemporal random fields to follow an autoregressive (AR1) process:

$$C_{s,t} \sim \text{Normal}\left(\mu_{s,t}, \sigma^2\right), \tag{7}$$

$$\mu_{s,t} = \mathrm{X}_{s,t}\beta + \omega_s + x_{s,t}, \tag{8}$$

$$\boldsymbol{\omega} \sim \text{MVNormal}\left(0, \mathbf{\Sigma}_\omega\right), \tag{9}$$

$$\mathrm{x}_{t=1} \sim \text{MVNormal}(0, \mathbf{\Sigma}_\varepsilon), \tag{10}$$

$$\mathrm{x}_{t>1} = \rho \mathrm{x}_{t-1} + \sqrt{1-\rho^2}\boldsymbol{\varepsilon}_t,\ \boldsymbol{\varepsilon}_t \sim \text{MVNormal}\left(0, \mathbf{\Sigma}_\varepsilon\right). \tag{11}$$

Here $C_{s,t}$ represents the climate variable (bottom temperature or log DO) in space s and time t, μ represents the mean, and σ represents the observation error standard deviation. The symbol $\mathrm{X}_{s,t}$ represents a vector of predictors (described below) and β represents a vector of corresponding parameters. The spatial random effects ω_s were defined as in Equation 5 whereas the spatiotemporal random effects were structured to follow a stationary AR1 process with first-order correlation ρ. Because DO is known to be influenced by both water temperature and seasonal biological processes, we included a quadratic effect for temperature and a linear effect for day of year along with estimated means for each year. Although not shown above for simplicity, we again allowed the quadratic depth covariates to follow a random walk through time as in Equation 3. Our bottom temperature model fixed effects included only depth and estimated means for each year, because including day of year did not improve model fit based on AIC (Akaike Information Criterion). Because bottom temperature data (but not DO) have been collected in synoptic surveys since 2003, we included these earlier data in the temperature model to provide more information for estimating the fixed spatial random field ω_s.

For all climate and biomass models, we then projected the model predictions onto a 4 × 4 km grid (UTM 9 projection) representing the survey domain. We excluded all cells with predicted conditions outside the range of conditions observed during sampling (99% quantiles of 3.07 to 11.3°C and 0.28 to 7.06 ml/L DO). We then calculated gradient-based velocities of change and constituent local trends and spatial gradients for each cell (see Methods S3 for discussion of alternative velocity calculation). Gradient velocities (V) were calculated as a ratio of the temporal trend (linear regression slope of each cell's climate time series) divided by gradient in space g of variable A,

$$V_s = \left(\Delta A_s / \Delta t\right) / g_s, \tag{12}$$

where A is any temporally varying feature of focal cell s. Depending on the portion of the survey grid considered, we calculated the trend through time for biennial time-steps between 2008 and 2018 (6 surveys across 11 years) or 2009 and 2017 (5 surveys across 9 years). In order to compare between survey areas with different sampling years, we converted values for all cells to a rate of change, or trend, per decade (Table 1). The spatial gradient g_s was calculated as the vector sum of the mean north–south and east–west gradients based on a 3 × 3 cell neighbourhood (Burrows et al., 2011); however, the values of A from which a spatial gradient is calculated can be based on any particular subset of times t, or the mean of all Δt. The input information related to a cell and any cell near enough to share spatial information in a gradient or in the overall spatial models (this includes all response and predictor variables) all share the same sample years.

The magnitudes of gradients g_s strongly influence the distribution of velocities V. Most prior applications of gradient-based velocities have used g_s calculated from the mean cell conditions of the entire period analyzed (e.g. Burrows et al., 2011; Molinos et al., 2019). Estimated velocities will tend to be larger (as $g_s \to 0$, $V_s \to \infty$) when more estimates (in this case sample years) are averaged for the cells included in the g_s calculation, because a larger sample reduces the

variability between the mean values of adjacent cells. Furthermore, the gradients most relevant to the actual distance a population would need to travel are those present after changes have begun to occur. Given that samples were collected only once every two years and that there is variability among species in terms of when dispersal occurs and how long it takes, we used the last two sample periods in our estimates of spatial gradients (2015–2018). This time period begins the first survey season following the onset of the 2014–2016 marine heat wave in the north-eastern Pacific (Peterson et al., 2015) and is approximately the end point of the transition to warmer conditions in the Bering sea (Alabia et al., 2018). We calculated spatial gradients using the `VoCC` R package (Brown & Schoeman, 2018), which we verified to produce identical results when applied to the same data as the newer package `VoCC` (García Molinos et al., 2019). Finally, we collapsed the most extreme velocity estimates to their 0.005 and 0.995 quantiles to reduce the impact of outliers from the resulting heavy-tailed distributions.

2.4 | Linking biotic changes with climate

To explore the relationship between change in estimated local climate and changes in estimated biomass densities for each 4 × 4 km grid cell, we used similar spatial GLMMs to control for spatial autocorrelation among cells. Our models estimated the rate of change in biomass (Y) of each maturity class of each species as a function of local climate change (temperature and DO) and an interaction between the mean climate of each cell and its local rate of change:

$$\Delta Y_{k[s]} \sim \text{Normal}\left(\mu_{k[s]}, \sigma^2\right), \tag{13}$$

$$\begin{aligned}\mu_{k[s]} = {} & \beta_{0,k[s]} + \beta_{1,k[s]}\overline{T}_s + \beta_{2,k[s]}\Delta T_s + \beta_{3,k[s]}\overline{T}_s\Delta T_s + \\ & \beta_{4,k[s]}\overline{O}_s + \beta_{5,k[s]}\Delta O_s + \beta_{6,k[s]}\overline{O}_s\Delta O_s + \beta_{7,k[s]}\overline{Y}_{k[s]} + \omega_{k[s]},\end{aligned} \tag{14}$$

$$\boldsymbol{\omega}_k \sim \text{MVNormal}\left(0, \boldsymbol{\Sigma}_\omega\right), \text{ for } k = 1, \cdots, K, \tag{15}$$

$$\beta_{r,k} \sim \text{Normal}\left(\eta_{r,k}, \sigma^2_{\beta_r}\right), \text{ for } k = 1, \cdots, K \text{ and } r = 0, \cdots, 7, \tag{16}$$

where $\overline{T}_s$ and ΔT_s represent the mean temperature and decadal trend in temperature for spatial location s. A row of data represents a given spatial grid cell s and species-maturity k combination. The symbols $\overline{O}_s$ and ΔO_s represent mean dissolved oxygen and decadal trend in dissolved oxygen, and the symbol $\overline{Y}_{k[s]}$ represents log biomass density for species-maturity k. Parameters β_0 through β_7 (indexed by r) represent coefficients that are allowed to vary as random effects across species with means $\eta_{r,k}$ and variances $\sigma^2_{\beta_r}$. We accounted for spatial autocorrelation through the spatial random effects $\omega_{k[s]}$, which follow a Matérn Gaussian Markov random field as described above.

We fit model configurations where both biomass and climate were calculated as either raw temporal trends or gradient-based velocities. The trend-based models assessed whether biomass changes were correlated with changes in climate at the 4 × 4 km grid cell scale. The velocity-based models assessed whether changes in biomass, especially those with low local variability in biomass, were correlated with the predicted speed of climate isoclines within the 12 × 12 km neighbourhood of cells. We did not include both trends and velocities in the same model because both the units and spatial scales captured are different.

For each maturity class of each species, we selected all grid cells that encompassed 95% of the mean total biomass across all sample years, and we included the mean log biomass density of each cell as a covariate to reduce the influence of changes occurring only at either the highest or lowest densities for a particular species. These models used a 600 knot mesh, Gaussian observation errors when estimating trends, and Student t-observation errors (with a degrees of freedom fixed at 7) to account for heavy-tailed residuals when estimating velocities. We scaled all covariates by their standard deviations. We centred local average temperature, DO, and log biomass density by their overall means, but kept temperature and DO trend variables uncentred to maintain interpretability. We tested additional covariates, including maturity class and local changes in fishing intensity, but we have not included them in the final models because they did not change our conclusions (see Methods S4).

2.5 | Simulation study

We conducted a simulation study to assess: (a) the ability of the geostatistical models to cope with the high levels of spatial covariance inherent in spatial grid-based climate and biomass estimates and (b) to what extent similarities in climate and biotic spatial gradients were responsible for the observed patterns in the velocity-based models. We simulated biomass trends for each species as random fields using the true variance and spatial correlation parameters estimated for each species. Next, we assessed how well our trend-based model accounted for spatial autocorrelation among grid-based estimates by re-fitting the trend-based model using four unique iterations of the simulated data and contrasting the effect sizes and number of species that showed a significant relationship with climate trends in the observed versus simulated models. If the spatial random effects were effective in preventing type I errors, the trend-based models using simulated data should not show a significant effect of climate more than expected by chance. In the case of velocities, we used the ratio of the simulated biomass trends to the observed spatial gradients in biomass to simulate biotic velocities (henceforth, 'time-null' velocities). This approach maintains the relationships between spatial gradients in biomass and climate that are likely to occur because both species abundances and climate on the seafloor are correlated with depth. Rather than being a test of spatial autocorrelation, these time-null velocities were used to test how important the gradient component was to the results of the fitted velocity model.

Null models based on simulated biotic trends and observed climate trends showed fewer significant relationships at the species-level than would be expected by chance (Figures S5–S7), confirming that the spatial random effects in our models (e.g. Figure S8) successfully controlled for the spatial autocorrelation.

In contrast, models predicting time-null biotic velocities did produce more significant effects than would be expected by chance (Figures S9–S11 versus S12). These associations were likely due to the simulated velocities being based on the observed spatial gradients (Figure S13); however, comparisons between the velocity model and time-null models suggest that some patterns cannot be accounted for by similarities in the spatial gradients and can be reliably attributed to variation in temporal trends (differences between areas encompassed in black versus grey violins for interaction terms in Figure 2b). This is in contrast to the complete overlap in black and grey violins for DO velocity in Figure 2b, which indicates that any set of species with identical overall distributions and population variability, but completely random biomass trends, would be likely to show just as many significant species-specific effects. Taken together, these simulations suggest that the velocity model effectively combines both the temporal and spatial dimensions of biotic and climate change, which provides support for our choice to focus on this approach.

2.6 | Life-history and ecological correlates of climate sensitivity

To assess potential ecological mechanisms and the extent to which the temporal and spatial scales considered were appropriate for the different species, we used mixed-effect models to assess concordance between species' life-history traits and ecology and the estimated effect of climate velocity. We first assessed the independent effects of mean population age (among immature populations only) and occupied depth (mean and range). We then tested for independent relationships between climate sensitivity and ecological groupings (including range limits, foraging zones, trophic level and sociality), while controlling for the depth total ranges occupied (see Methods S5).

3 | RESULTS

3.1 | Climate trends and velocities

We estimated bottom temperature and DO values biennially between late May and early August during 2008–2018 or 2007–2019, depending on the surveyed area. Seafloor temperature varied from 4.6 to 10.2°C (95% quantile range) across 4 × 4 km grid cells that had a mean depth within the 99th quantile range of sampled depths (23–1,112 m). For the same range of survey depths, DO ranged between 0.7–5.7 ml/L (95% quantiles). For both temperature and DO, the highest values were associated with the shallowest depths, while the lowest values were associated with the deepest locations (Figure 1b, c).

Over this period, summer seafloor temperature increased by an average of 0.6°C per decade across the entire region (95% quantile range −0.2–1.8°C per per decade; Figure 1d). In contrast, the direction of change in seafloor DO was more variable (95% quantiles: −2.8–0.6 ml/L per decade; Figure 1e).

Warming tended to be most pronounced in the already warmer locations—mean of 1.3°C/decade in cells shallower than 50 m (Figure S14b). Likewise, the greatest decreases in DO occurred in the shallowest locations (mean: −2 ml/L per decade); however, the highest variability in DO trend (95% quantiles: −1.7 to 0.6 ml/L per decade) occurred between 50 and 200 m depths (Figure S14e). There was a tendency for the shallowest depths to be occupied by groundfish species that have narrower depth ranges (e.g. Southern Rock Sole (*Lepidopsetta billineta*, Pleuronectidae) versus Dover Sole (*Microstomus pacificus*, Pleuronectidae); Figure S14g; Table S1).

When these local climate trends were placed in their geographic context by converting to gradient-based velocity estimates (Equation 12), they implied that a population would have to move an average of 10.5 km/decade (mean of absolute values) to maintain its starting thermal environment and an average of 11 km/decade to maintain initial DO levels. Temperature velocities averaged positive, representing warming conditions (mean: 10.1, 95% interquantile range of −12 to 87; Figure 1f), while DO velocities averaged negative, representing declining DO levels (−6.26, −91 to 24; Figure 1g). Most locations with high climate velocities occurred in patches throughout Queen Charlotte Sound and Hecate Strait (dark red patches in Figure 1f). The most negative DO velocities occurred in shallower portions of Hecate Strait (largest green patch in Figure 1g). The largest velocities tended to be found across a broader range of depths than the largest climate trends (Figure S14).

3.2 | Linking biotic changes with climate

Geostatistical models linking climatic (Figure 1d-g) and biotic trends (Figures S17 and S18) or velocities (Figures S19 and S20) resolved different aspects of biotic change (Figures S8 and S12). The effect of temperature velocity on biotic velocity was weakly positive across species (β: 0.28 km/decade with 95% CI −0.04 to 0.60; point range for "T change" shown in Figure 2b), despite a significant overall 0.55% decline in biomass (−0.87 to −0.22) per 1 *SD* increase in warming (0.8°C per decade) based on local temperature trend only (point range for "T change" shown in Figure 2a). However, mean local temperature influenced the effect of temperature velocity on biotic velocity (β: −1.09, −1.48 to −0.70; "T interaction" in Figure 2b), such that when temperature velocity was high in the warmest parts of a species' range, local biomass was more likely to decline and exhibit larger negative or smaller positive biotic velocities. When temperature velocity was high in the coolest parts of a species range, local biomass was more likely to increase and to result in larger positive biotic velocities (or to decrease less and result in less negative biotic velocities).

Interactions between mean climate and climate velocity for each maturity class of each species can be illustrated as the predicted relationships between climate and biotic velocities at different mean local conditions (e.g. in Figure 3c and S15a, the blue and red lines are the predicted relationships for locations at the 0.025 and 0.975 quantile of mean local temperatures, respectively). For Redbanded Rockfish (*S. babcocki*) the horizontal blue line indicates stable biomass (small

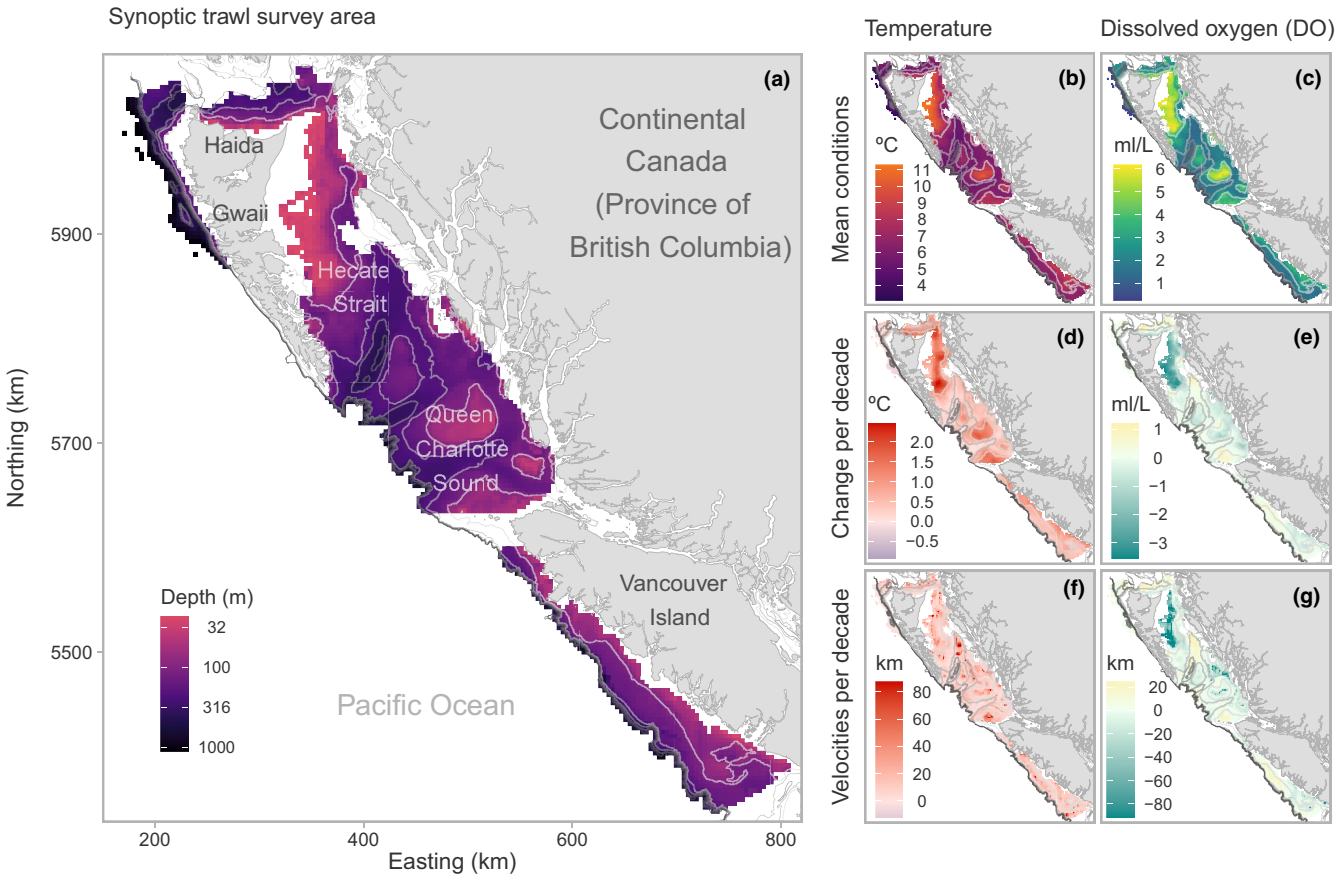

FIGURE 1 Maps of study area (a), predicted mean conditions (b, c), decadal trends (d, e), and decadal velocities (f, g) of bottom temperature and dissolved oxygen (DO) for 2008-2018 off the coast of British Columbia, Canada (UTM zone 9). Values are estimated using geostatistical spatiotemporal models of CTD sensor data collected during late-spring/early-summer groundfish trawl surveys. Bathymetry lines at every 100 m are overlaid in shades of grey that increase with depth

absolute biotic velocities), while the red line with a negative slope means that biomass was more likely to be declining across a local area where conditions were warmest on average and getting warmer across more of the surrounding area (Figure 3b). The slopes of all predicted relationships (e.g. as illustrated in Figure 3c and Figure S15a) are plotted for all species-maturity combinations in Figure 4. Consistent with the overall interaction, the majority of species-maturity combinations with significant interactions between local mean temperature and temperature velocity had negative interactions (31 of 33 coloured dots and lines with red coefficients to the left of blue coefficients in Figure 4a). Over a third of these cases predicted a positive effect of increased temperature velocities for both the warmest and coolest locations, but this relationship was more strongly positive in the cooler locations (13 of 31 species-maturity combinations with negative interactions).

To assess whether these relationships predicted specific species' biotic velocities to have increased or decreased under different climate velocities, the lines displayed in Figure 3c and S15a can be "sliced" at either the minimum temperature velocity experienced by each species (left end of lines) or at the maximum (right end of lines). The expected biotic velocity was near-zero for most species-maturity combinations in locations experiencing minimum climate velocity (Figure 5a) regardless of mean temperature. However, in the warmest locations experiencing maximum climate velocity, the expected biotic velocity was strongly negative for 19 of 69 species-maturity combinations (Figure 5b). Meanwhile, in cooler locations experiencing the same high climate velocity, biotic velocities were often positive (e.g. Pacific Halibut, *Hippoglossus stenolepis*, Pleuronectidae).

After controlling for temperature, the average effect of DO velocity on biotic velocity was negative across species (β: −0.48 km/decade, −0.82 to −0.15; point and range for "DO change" in Figure 2b) despite there being a positive effect of DO trend on biomass trend (β: 0.34% increase in biomass, 0.16 to 0.52; point and range for "DO change" in Figure 2a). Thus, while increasing DO was associated with increases in biomass at a local scale, DO velocity was not on average correlated with biotic velocities. However, unlike for temperature, DO velocity did not interact with mean DO availability consistently across species (β: 0.25, −0.05 to 0.55). Only two species (those with green point ranges on the positive side of the x-axis in Figure 4b) showed the expected interaction where locations with lower mean DO levels experiencing positive DO velocities were associated with increases in biotic velocity and/or negative DO velocities were associated with decreases in biotic velocity (e.g. immature Lingcod, *Ophiodon elongatus*, Hexagrammidae; Figure 3). In contrast, several species experienced declines in biotic

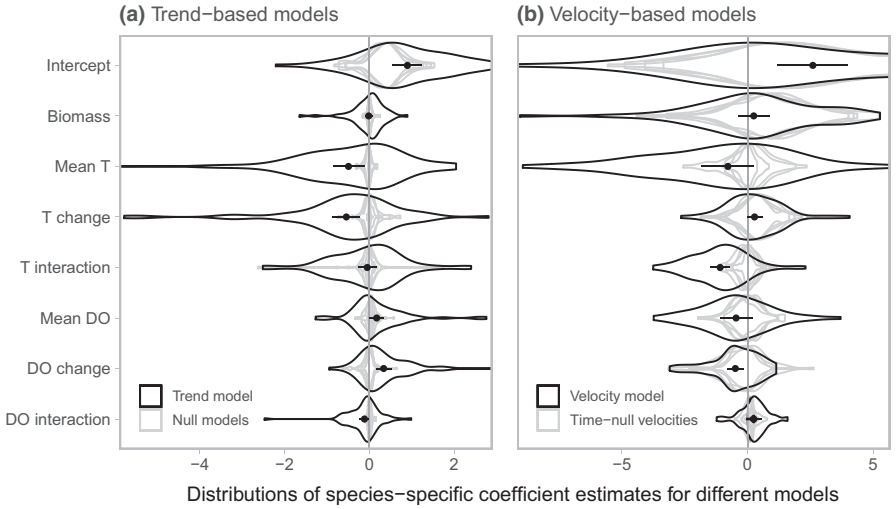

FIGURE 2 Distribution of species-specific (random effect) coefficients from the model fitted to the observed data (black violins) compared with coefficients from four simulated null models (grey violins). Each "violin" is based on a single model including all species: (a) trend-based models where climate and biotic change variables are all local trends and (b) velocity models where climate and biotic change variables are all velocities. Black points with ranges represent the observed data global (fixed effect) coefficient estimates with 95% CIs. Null models used fitted covariate values, but simulated response data. Simulated time-null velocities used these same simulated trends divided by the real spatial gradients. The x-axes have been truncated slightly for interpretability

velocity when DO velocity increased across the range of mean DO levels (black point ranges on negative side of x-axis in Figure 4b). Including DO in the model along with temperature did not substantially alter the effects of temperature for any species (Figure S16).

3.3 | Life-history and ecological correlates of climate sensitivity

We examined possible relationships between responses to climate velocities and each species' taxonomy, traits and depth distributions. Relationships with biotic velocities that were negative at high temperatures or positive at low temperatures occurred in members of both the largest families represented in our analysis, Sebastidae (rockfish) and Pleuronectidae (righteye flounders) suggesting no strong patterns of similarity among species belonging to the same genus or family (Figure 4a and S12; see also non-significant family-level effects from hierarchical model, Figure S21). However, the effects of temperature velocities at high temperatures were most negative for Chondrichthyan biotic velocities (−1.8 km/decade per *SD* in temperature velocity, same units apply elsewhere) and rockfish species occupying shelf habitats (−1.3), neutral for continental slope rockfish (0.1) and flatfish (−0.1), and most positive for Sablefish (1.0; mean across red values in Figure 4a).

Life-history failed to explain substantial variation in climate sensitivity in the warmest locations, although more negative effects tended to be clustered in shallow depths and among younger immature populations (Figure S22). However, immature populations did not have overall stronger responses than mature populations (Figure S23b). The positive effects of temperature velocities on biotic velocities in the coolest locations were strongest in species occupying a larger range of depths (β: 0.57, 0.21 to 0.92) and for immature populations with younger mean age (β: −1.0, −2.0 to 0.0). Ecological factors were somewhat better at accounting for negative effects in the warmest locations. The effects of temperature velocity at high mean temperatures differed significantly between species depending on diet (lower biotic velocities in zooplanktivores than species at higher trophic levels; β: −0.96, −1.44 to −0.48), and use of foraging zones (higher biotic velocities in demersal species relative to benthopelagic; β: 0.98, 0.47 to 1.49) after accounting for mean depth occupied (Figure S24 top row). The strongest negative effects of warming temperature velocities (estimated for the warmest parts of a species distribution) were for species occurring at intermediate depths, whereas most species with mean encounter depths deeper than 290 m appeared to increase in biotic velocity with more positive temperature velocities (Figure S25c).

In contrast, DO velocities at low mean DO locations only showed a strong positive effect on Lingcod biotic velocities (0.7) and negative effects were strongest for both continental slope rockfish (−1.1) and flatfish (−1.4; mean across green values in Figure 4b). These negative relationships represent declining biotic velocity with increasing DO, or vice versa, and tended to be stronger both for species occupying deeper locations on average (β: −0.43, −0.73 to −0.13; Figure S25d) and a larger range of depths (β: −0.30, −0.60 to 0.0). It is notable, however, that the effect of trends in DO on per cent change in biomass were also negative at these depths despite being mostly positive at intermediate depths (Figure S25b). At these intermediate depths (the mean occupied depth for species in this analysis of about 175 m), the effects of DO velocity at low DO was also most negative for species foraging at higher trophic levels (β: −0.33, −0.81 to 0.16), in the demersal zone (β: −0.79, −1.32 to −0.26), and with more solitary habits (β: −0.63, −1.21 to −0.06; Figure S24 bottom row).

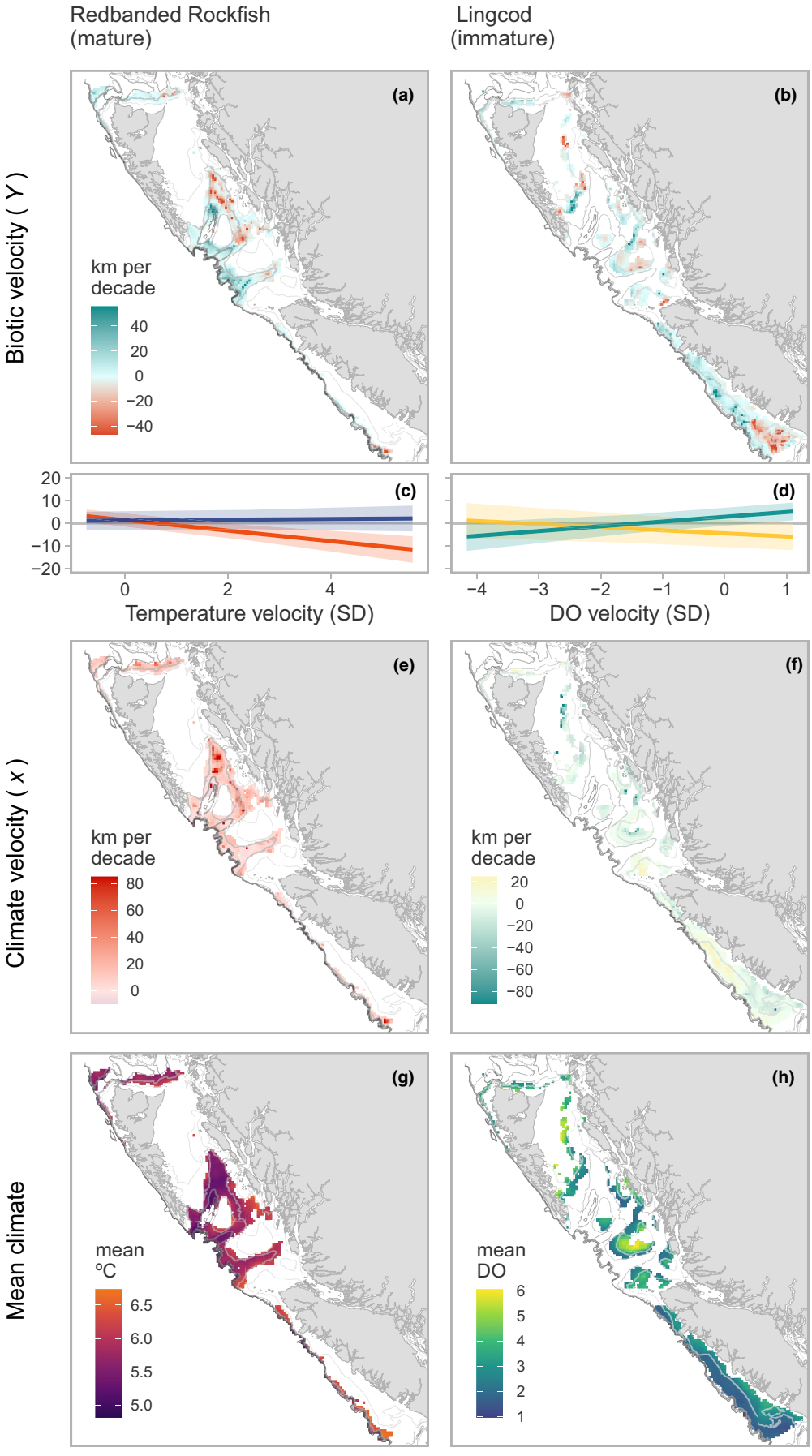
Redbanded Rockfish
(mature)
Lingcod
(immature)
Biotic velocity (Y)
(a)
(b)
km per
decade
40
20
0
−20
−40
(c)
(d)
20
10
0
−10
−20
0
2
4
Temperature velocity (SD)
−4
−3
−2
−1
0
1
DO velocity (SD)
Climate velocity (x)
(e)
(f)
km per
decade
80
60
40
20
0
km per
decade
20
0
−20
−40
−60
−80
Mean climate
(g)
(h)
mean
°C
6.5
6.0
5.5
5.0
mean
DO
6
5
4
3
2
1

FIGURE 3 Maps and interaction plots for two illustrative species representing the most frequent relationship with temperature (left column) and the expected response with DO (right column). Mature Redbanded Rockfish had stable, near-zero, biotic velocities regardless of amount of warming in the coolest regions it occupied, and decreases in biomass when temperatures increased in warmer regions (a,c,e,g). Immature Lingcod biotic velocities increased with positive DO velocities in low mean DO locations only (b,d,f,h). In panel c, a blue line represents predicted biotic velocity (*y*, y-axis) for different temperature velocities (*x*, x-axis) in the coolest locations (0.025 quantile of those occupied by 95% of the estimated biomass of each species) and a red line represents the same for the warmest locations (0.975 quantile). Likewise, for predictions at different DO velocities, green represents the lower quantile of mean DO and yellow the higher (d). Both the colours and slopes illustrated correspond with those in Figure 4. The maps include biotic velocity estimates for all locations that cumulatively account for 95% of the estimated biomass of each species (a, b), and the same climate estimates as in Figure 1, but trimmed to include only the values for the same locations as the biotic velocities for each species

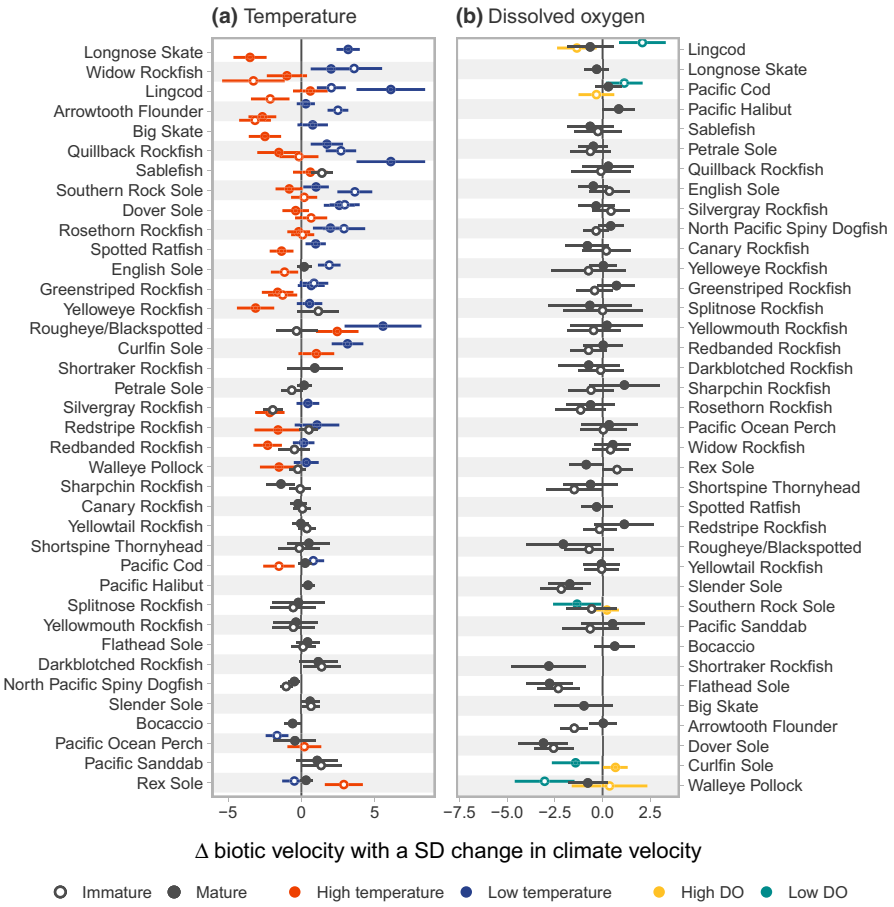

FIGURE 4 Mean climate and climate change interact in predicting biotic velocities (km/decade) for 38 groundfish species. Coloured dot-whiskers indicate slopes and 95% CIs of the predicted biotic velocities with 1 SD of change in climate velocity for the low and high 95% quantiles of mean local climate (i.e. the slopes of lines in interaction plots like those in Figure 3c, d). Species are ordered by the difference between the slopes at the highest and lowest quantiles of mean climate such that the more intuitive results are at the top: increases in climate velocity have a more positive impact on biotic velocity when starting at a low mean temperature (a) or DO level (b). Open circles indicate patterns for immature fish and closed circles represent individuals large enough to have a 50% chance of having reached reproductive maturity, or belonging to species for which maturity data was not available. Black dot-whiskers represent the slopes for each maturity class when the interaction is not significant. See Table S1 for scientific names

4 | DISCUSSION

Using novel geostatistical models fit to bottom temperature, DO, and demersal fish biomass from scientific trawl surveys, we related trends and velocities between climatic and biotic variables across 38 species. Local declines in demersal fish biomass were, on average, associated with warming trends and decreases in DO. However, after converting trends to velocities, a clear interaction between temperature velocity and mean bottom temperature emerged. On average, and for roughly half the species-maturity combinations, temperature velocity had a more negative effect on biotic velocity in already warm locations than in relatively cool locations. Converting these interaction effects into expected values, approximately one quarter of species-maturity combinations experienced declines (negative biotic velocities) in

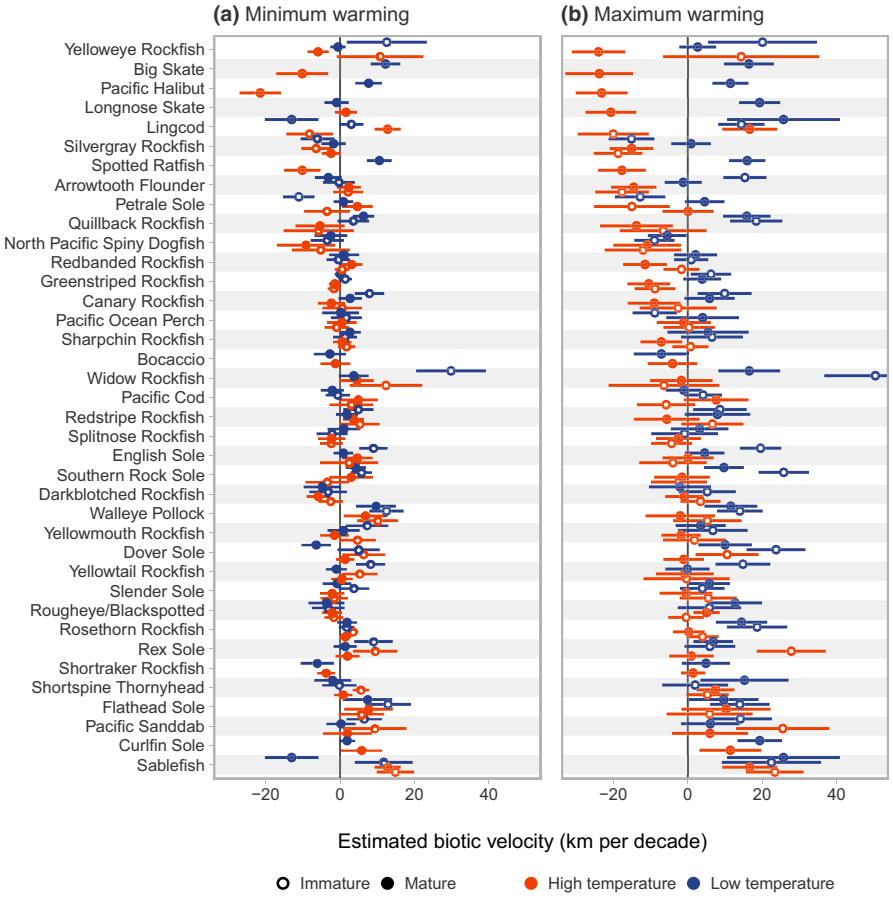

FIGURE 5 Estimates of biotic velocities (km/decade with 95% CI) for 38 groundfish species under different mean temperatures (blue and red represent low and high 95% quantiles) occupied and at (a) the minimum and (b) maximum temperature velocities experienced for each species. Open circles indicate patterns for immature fish and closed circles represent individuals large enough to have a 50% chance of being reproductively mature, or belonging to species for which maturity data were not available. Species are ordered by the minimum estimates at the maximum climate velocity experienced for each species. Therefore, species most likely to experience population declines with increasing temperatures are at the top

the warmest locations when experiencing maximum warming. In contrast, locations experiencing minimal warming or cool locations experiencing maximum warming experienced stable or increasing biotic velocities. Characteristics such as trophic level, foraging zone, and sociality—as well as potentially confounding variables such as commercial fishing effort or catch—explained little of the observed effects. Although DO velocity results were more equivocal, planktivores responded more positively to DO velocity under low DO conditions than species with more diverse or higher trophic-level diets. This suggests that the prevalence of strong negative relationships between DO and biotic velocities might be explained by increases in primary production, causing decreases in DO due to increased rates of decomposition in benthic environments (Keister et al., 2020).

4.1 | Scale and context dependence

Our analysis is the first, to our knowledge, to explore how the interaction between climate velocities and local mean climate conditions affect fine-scale biotic velocities, and the first to contrast patterns between trend and velocity indices. Relationships between climate and biotic velocities have also been detected in marine species in the Arctic (Alabia et al., 2018) and between local climate velocities and species range shifts in tropical to subarctic zones along the Japanese archipelago (Kumagai et al., 2018) and along several portions of the continental shelf of North America (Fredston-Hermann et al., 2020; Pinsky et al., 2013). At a global scale, the impact of temperature change in marine environments appears to be highly dependent on baseline conditions, whether measured in range shifts relative to temperature velocity (e.g. Lenoir et al., 2020) or species richness and abundance in response to temperature trends (e.g. Antão et al., 2020). Specifically, this latter meta-analysis of patterns in marine taxa found that abundance was positively correlated with warming, except in the warmest of locations (Antão et al., 2020). The wide geographic scope of these analyses suggest that our focus on both local climate velocity and baseline environmental conditions may be broadly relevant to explaining climate change induced range shifts in marine taxa in regions around the globe.

While our trend model indicated an overall negative effect of rising temperatures on local fish density, the velocity model included an interaction that showed that the strongest negative relationships occurred only in already warm locations. Large climate velocities reflect more spatially uniform environments—where a population would need to move greater distances to maintain constant climate—and likewise, small velocities reflect more spatially heterogeneous environments (Loarie et al., 2009). As a result, more spatially uniform regions have greater weight in the velocity model than in the trend model, and this stretching and compressing of trend values based on spatial heterogeneity likely explains why the negative interactive effect of mean temperature was only detected for velocities. Overall, we focused primarily on the velocity results since they represent a more ecologically meaningful measure than trends alone, given that

they account for the local reality species face if tracking a constant environment (Brito-Morales et al., 2018), or tracking prey that themselves track the environment.

For many species, we do not know how far individuals travel on a daily or seasonal basis, so uncertainty remains about the extent to which the modelled spatial and temporal resolutions are appropriate for each of the species in this analysis. While the trend- and velocity-based models capture slightly different spatial scales (4 × 4 km focal cell versus 12 × 12 km encompassed when considering patterns among neighbouring cells as well), both resolutions are finer than what is often used for analyses of climate change in the marine environment (Oestreich et al., 2020; Pinsky et al., 2020). Substantial environmental changes can occur at even fine scales, and these local-scale effects may be especially important for species with high site fidelity (e.g. Yelloweye Rockfish *S. ruberrimus*, Hannah & Rankin, 2011). However, in order to detect the impact of climate change on rockfish (many of which have generation times >20 yrs), one would require either data in excess of 20 years, or to contrast patterns of change between age classes. Indeed, responses to environmental change can be expected to differ between species, depending on the life history of species including physiological tolerances, lifespan, and dispersal patterns (Massiot-Granier et al., 2018). Furthermore, reaching reproductive maturity frequently results in shifts in dispersal patterns, habitat selectivity, physiological tolerances (Laurel et al., 2007), and therefore, represents a potentially important break point for understanding the impacts of climate change. Given the relatively short timescale encompassed in our analysis (one decade), we expected to find stronger patterns in shorter-lived/immature portions of populations and more pelagic species. Within immature populations, those with a younger mean age were found to exhibit the most extreme responses to temperature velocity, but not stronger responses than mature populations. Finally, both spatial and temporal scales of response could be complicated by interactions with depths occupied; but, contrary to expectation, more extreme responses tended to belong to demersal foraging and solitary species, rather than those with more pelagic or schooling behaviours.

Aggregate metrics such as the centre of gravity have also demonstrated that demersal fishes use both shifts in latitude and depth to track changes in ocean temperatures (e.g. Dulvy et al., 2008; Li et al., 2019; Perry et al., 2005), but evidence that range edges on the North American continental shelf have shifted further north than expected or even contracted southward, suggest roles for competition, climate-independent mortality and/or density-dependent habitat selection (Fredston et al., 2020; Li et al., 2019). Indeed, fishing pressure on the Atlantic shelf was found to be more important than average bottom temperature for predicting centre of gravity for five groundfish species, despite temperature being more correlated with variance in biomass (Adams et al., 2018). This latter result suggests that there was spatial variability in temperature, or responses to temperature, which were not fully captured by the centre of gravity (VanDerWal et al., 2013). Fine-scale local effects may contribute to the relatively greater influence of temperature relative to fishing pressure in our analysis. Groundfish species in the eastern Bering Sea also do not show a strong correlation between local climate and biotic velocities, but no interaction with mean conditions was reported (Alabia et al., 2018). Another potential explanation for stronger negative effects on Canadian Pacific groundfish is that species in this region are closer to the southern ends of their distributions than in Alaska and may, therefore, be closer to the warm end of their temperature tolerances, especially in the warmest locations. However, although we found the strongest negative biotic velocities in these warmer locations, species nearer to their northern range limit (designated by N under 'Range limit' in Table S1) were not more likely to show a positive response to temperature.

4.2 | Limitations and implications

There are a number of limitations to our analysis. First, our analysis cannot separate fish population movement in response to climate from a host of other possible explanations. For example, local changes in biomass density can be a result of movement, local population growth, age cohorts beyond our two maturity categories, changes in average body size (Laurel et al., 2007; Shackell et al., 2010), or effects of fishing not captured by the metrics of total catch or hours fished. Indeed, some of the hypothesized effects of warming climate and lower DO on fishes include higher metabolism and ability to store fat, reduced productivity, and slower growth resulting in generally smaller fish (Klein et al., 2017; Madeira et al., 2017). Furthermore, changes in local density may be correlated with climate, not because of groundfish thermal preference, but because groundfish seek prey or avoid predators that have themselves shifted their distribution in response to climate. Second, there are limitations to our data. The CTD climate data from Canadian Pacific trawl surveys are only available from 2008 onward, the surveys occur in one seasonal period (May to August) and cover a given region only once every two years. Also, some of the species (e.g. shallower rockfish species) may be better sampled by longline gear than trawl gear. This spatial and temporal scope will miss overlap in major life-history events for some species (e.g. Sablefish; Beamish, 2008), or seasonal movements (e.g. Pacific Halibut; Loher, 2011). Importantly, the input data for our meta-analytic model are predictions from our first-stage geostatistical models. Third, it is possible that climate conditions may themselves affect survey catchability. For example, groundfish may flee gear more slowly or aggregate to avoid low DO conditions (Craig, 2012), thereby making fish more catchable and biasing observations.

This analysis suggests multiple future research directions. First, future efforts may aim to identify common spatial patterns across species using spatial dimension reduction tools such as spatial factor analysis (Thorson, Scheuerell, et al., 2015). Areas where species overlap in their response would represent important areas for conservation (Brito-Morales et al., 2018), but also areas where competition may be expected to increase or new fisheries interactions may occur. Second, some rockfish are better sampled by longline survey gear and future analyses could use such survey data, or combine survey data from multiple gear types (Webster et al., 2020), to develop a composite density estimate. Third, our analysis used CTD

data, which was only available for spring or summer from 2008 onwards and required a statistical model to extrapolate to the full region. An alternative would be a ROMS (Regional Ocean Modeling System) model (Peña et al., 2019), which could extend the temporal scope, allow for accounting of climate at other times of the year (e.g. temperature during spawning; Laurel & Rogers, 2020), allow for inclusion of variables not typically measured with survey data (e.g. primary production), and allow for forward projections. Preliminary investigations indicated a strong correlation between our CTD projections and recently updated ROMS bottom temperatures. With the greater spatial and temporal extent that ROMS data will provide, calculation of more geographically precise analogue-based climate velocities could be used to further refine the identification of areas important for conservation (Brito-Morales et al., 2018).

The spatial shifts we identified could have a number of management consequences. First, we observed changes over a decade and such redistribution is likely to compound over time. Redistribution can impact fishing opportunities and conservation of rarer species when "choke" species (species with limited quota that co-occur with species of fishing interest) limit fishing opportunities (e.g. Forrest et al., 2020). Redistribution can also impact nations or peoples with relatively small defined spatial fishing rights and have consequences for marine spatial planning. For example, a marine reserve designed to protect a particular at-risk population may no longer be as effective after a local redistribution of abundance. Lastly, shifting distributions can affect calculation of indices of abundance, and estimates of stock size and stock status, which in turn may impact harvest recommendations (Karp et al., 2019; Szuwalski & Hollowed, 2016).

Climate change is expected to have large impacts on fish stocks and their management, particularly with respect to changes in species distribution (e.g. Free et al., 2019; Karp et al., 2019; Tommasi et al., 2017). Legislation and policy in jurisdictions around the world (e.g. the US *Magnuson-Stevens Act*, Canada's *Fisheries Act*, the European *Marine Strategy Framework Directive*) require that environmental conditions affecting fish stocks be accounted for in management decisions such as setting sustainable catch limits and developing rebuilding plans. However, there is often a mismatch between scale of climate predictions, the scale at which species respond, and the scale of management decisions (Maureaud et al., 2021; Stock et al., 2011). For example, the populations analysed in this study are managed at the mesoscale, with catch limits often determined for individual substocks (DFO, 2019). The metrics presented in our paper represent fine-scale indicators of response to a changing environment, which are useful for assessing risk and conservation planning (Brito-Morales et al., 2018). Analyses such as ours can be incorporated into frameworks for improving advice for the management of fisheries under climate change (e.g. Karp et al., 2019; Plagányi et al., 2011; Punt et al., 2014).

ACKNOWLEDGEMENTS

We thank Fisheries and Oceans Canada's Aquatic Climate Change Adaptation Services Program (ACCASP) for funding that supported this work. We thank E.A. Keppel, G.D. Workman, and M.R. Wyeth for helpful discussions and assistance with data extraction. We thank P.L. Thompson and three anonymous reviewers for comments that substantially improved this manuscript. We thank the many individuals who have contributed to collecting and curating the synoptic survey data on which this manuscript is based.

DATA AVAILABILITY STATEMENT

The biological data that used in this study are openly available through open.canada.ca at https://open.canada.ca/data/en/dataset/a278d1af-d567-4964-a109-ae1e84cbd24a and associated environmental measurements are available from https://www.pac.dfo-mpo.gc.ca/stats/index-eng.html. All of the code underlying this analysis is available at https://github.com/pbs-assess/gfvelocities.

ORCID

Philina A. English https://orcid.org/0000-0003-2992-6782
Eric J. Ward https://orcid.org/0000-0002-4359-0296
Robyn E. Forrest https://orcid.org/0000-0002-7709-213X
Luke A. Rogers https://orcid.org/0000-0003-3843-064X
Andrew M. Edwards https://orcid.org/0000-0003-2749-8198
Sean C. Anderson https://orcid.org/0000-0001-9563-1937

REFERENCES

Adams, C. F., Alade, L. A., Legault, C. M., O'Brien, L., Palmer, M. C., Sosebee, K. A., & Traver, M. L. (2018). Relative importance of population size, fishing pressure and temperature on the spatial distribution of nine Northwest Atlantic groundfish stocks. *PLoS One*, *13*, e0196583. https://doi.org/10.1371/journal.pone.0196583

Alabia, I. D., Molinos, J. G., Saitoh, S. I., Hirawake, T., Hirata, T., & Mueter, F. J. (2018). Distribution shifts of marine taxa in the Pacific Arctic under contemporary climate changes. *Diversity and Distributions*, *24*, 1583–1597. https://doi.org/10.1111/ddi.12788

Anderson, S. C., Keppel, E. A., & Edwards, A. M. (2019). A reproducible data synopsis for over 100 species of British Columbia groundfish. *DFO Canadian Science Advisory Secretariat Research Document*. **2019/041**. Available from https://www.dfo-mpo.gc.ca/csas-sccs/Publications/ResDocs-DocRech/2019/2019_041-eng.html

Anderson, S. C., Ward, E. J., English, P. A., & Barnett, L. A. K. (2020). *sdmTMB: Spatiotemporal Species Distribution GLMMs with 'TMB'*. Available from https://github.com/pbs-assess/sdmTMB . R package version 0.0.11.9000

Antão, L. H., Bates, A. E., Blowes, S. A., Waldock, C., Supp, S. R., Magurran, A. E., Dornelas, M., & Schipper, A. M. (2020). Temperature-related biodiversity change across temperate marine and terrestrial systems. *Nature Ecology and Evolution*, *4*, 927–933. https://doi.org/10.1038/s41559-020-1185-7

Barbeaux, S. J., & Hollowed, A. B. (2018). Ontogeny matters: Climate variability and effects on fish distribution in the eastern Bering Sea. *Fisheries Oceanography*, *27*, 1–15. https://doi.org/10.1111/fog.12229

Beamish, R. J. (2008). Impacts of climate and climate change on the key species in the fisheries in the North Pacific. *North Pacific Marine Science Organization Scientific Report* 35

Bell, R. J., Odell, J., Kirchner, G., & Lomonico, S. (2020). Actions to promote and achieve climate-ready fisheries: Summary of current practice. *Marine and Coastal Fisheries*, *12*, 166–190. https://doi.org/10.1002/mcf2.10112

Brito-Morales, I., García Molinos, J., Schoeman, D. S., Burrows, M. T. et al (2018). Climate velocity can inform conservation in a warming world. *Trends in Ecology & Evolution*, *33*, 441–457. https://doi.org/10.1016/j.tree.2018.03.009

Brown, C., & Schoeman, D. (2018). *vocc: Functions for Calculating the Velocity of Climate Change*. Available from https://github.com/cbrown5/vocc . R package version 0.1.1

Burrows, M. T., Schoeman, D. S., Buckley, L. B., Moore, P. et al (2011). The pace of shifting climate in marine and terrestrial ecosystems. *Science*, *334*, 652–655. https://doi.org/10.1126/science.1210288

Carroll, C., Lawler, J. J., Roberts, D. R., & Hamann, A. (2015). Biotic and Climatic Velocity Identify Contrasting Areas of Vulnerability to Climate Change. *PLoS One*, *10*, e0140486. https://doi.org/10.1371/journal.pone.0140486

Comte, L., & Grenouillet, G. (2015). Distribution shifts of freshwater fish under a variable climate: Comparing climatic, bioclimatic and biotic velocities. *Diversity and Distributions*, *21*, 1014–1026. https://doi.org/10.1111/ddi.12346

Craig, J. K. (2012). Aggregation on the edge: Effects of hypoxia avoidance on the spatial distribution of brown shrimp and demersal fishes in the Northern Gulf of Mexico. *Marine Ecology Progress Series*, *445*, 75–95. https://doi.org/10.3354/meps09437

Cressie, N. A. C., & Wikle, C. K. (2011). *Statistics for Spatio-Temporal Data*. Wiley Series in Probability and StatisticsWiley.

DFO (2019). Pacific region integrated fisheries management plan, groundfish, effective February 21, 2019, version 1.1. Available from http://www.pac.DFO.mpo.gc.ca/fm-gp/mplans/ground-fond-ifmp-pgip-sm-eng.html

DFO (2020). Groundfish Synoptic Bottom Trawl Surveys - Open Government Portal. Available from https://open.canada.ca/data/en/dataset/a278d1af-d567-4964-a109-ae1e84cbd24a

Doney, S. C., Ruckelshaus, M., Emmett Duffy, J., Barry, J. P. et al (2012). Climate change impacts on marine ecosystems. *Annual Review of Marine Science*, *4*, 11–37. https://doi.org/10.1146/annurev-marine-041911-111611

Dulvy, N. K., Rogers, S. I., Jennings, S., Stelzenmller, V., Dye, S. R., & Skjoldal, H. R. (2008). Climate change and deepening of the North Sea fish assemblage: A biotic indicator of warming seas. *Journal of Applied Ecology*, *45*, 1029–1039. https://doi.org/10.1111/j.1365-2664.2008.01488.x

Dunn, P. K., & Smyth, G. K. (2005). Series evaluation of Tweedie exponential dispersion model densities. *Statistics and Computing*, *15*, 267–280. https://doi.org/10.1007/s11222-005-4070-y

Forrest, R. E., Stewart, I. J., Monnahan, C. C., Bannar-Martin, K. H., & Lacko, L. C. (2020). Evidence for rapid avoidance of rockfish habitat under reduced quota and comprehensive at-sea monitoring in the British Columbia Pacific halibut fishery. *Canadian Journal of Fisheries and Aquatic Science*, *77*, 1409–1420. https://doi.org/10.1139/cjfas-2019-0444

Fredston, A., Pinsky, M., Selden, R., Szuwalski, C., Thorson, J., Halpern, B., & Gaines, S. (2020). Range edges of North American marine species are tracking temperature over decades. Preprint. https://doi.org/10.22541/au.160331933.33155622/v1

Fredston-Hermann, A., Selden, R., Pinsky, M., Gaines, S. D., & Halpern, B. S. (2020). Cold range edges of marine fishes track climate change better than warm edges. *Global Change Biology*, *26*, 2908–2922. https://doi.org/10.1111/gcb.15035

Free, C. M., Thorson, J. T., Pinsky, M. L., Oken, K. L., Wiedenmann, J., & Jensen, O. P. (2019). Impacts of historical warming on marine fisheries production. *Science*, *363*, 979–983. https://doi.org/10.1126/science.aau1758

Frölicher, T. L., Fischer, E. M., & Gruber, N. (2018). Marine heatwaves under global warming. *Nature*, *560*, 360–364. https://doi.org/10.1038/s41586-018-0383-9

Frölicher, T. L., & Laufkötter, C. (2018). Emerging risks from marine heat waves. *Nature Communications*, *9*, 650. https://doi.org/10.1038/s41467-018-03163-6

García Molinos, J., Halpern, B., Schoeman, D., Brown, C., Kiessling, W., Moore, P. J., Pandolfi, J. M., Poloczanska, E. S., Richardson, A. J., & Burrows, M. T. (2016). Climate velocity and the future global redistribution of marine biodiversity. *Nature Climate Change*, *6*, 83–88. https://doi.org/10.1038/nclimate2769

García Molinos, J., Schoeman, D. S., Brown, C. J., & Burrows, M. T. (2019). *VoCC: The Velocity of Climate Change and related climatic metrics*. Available from https://doi.org/10.5281/zenodo.3382092. R package version 1.0.0

Godefroid, M., Boldt, J. L., Thorson, J. T., Forrest, R., Gauthier, S., Flostrand, L., Ian Perry, R., Ross, A. R. S., & Galbraith, M. (2019). Spatio-temporal models provide new insights on the biotic and abiotic drivers shaping Pacific Herring (*Clupea pallasi*) distribution. *Progress in Oceanography*, *178*, 102198. https://doi.org/10.1016/j.pocean.2019.102198

Hamann, A., Roberts, D. R., Barber, Q. E., Carroll, C., & Nielsen, S. E. (2015). Velocity of climate change algorithms for guiding conservation and management. *Global Change Biology*, *21*, 997–1004. https://doi.org/10.1111/gcb.12736

Hannah, R. W., & Rankin, P. S. (2011). Site fidelity and movement of eight species of Pacific rockfish at a high-relief rocky reef on the Oregon coast. *North American Journal of Fisheries Management*, *31*, 483–494. https://doi.org/10.1080/02755947.2011.591239

Hare, J. A., Alexander, M. A., Fogarty, M. J., Williams, E. H., & Scott, J. D. (2010). Forecasting the dynamics of a coastal fishery species using a coupled climate–population model. *Ecological Applications*, *20*, 452–464. https://doi.org/10.1890/08-1863.1

Karp, M. A., Peterson, J. O., Lynch, P. D., Griffis, R. B., Adams, C. F., Arnold, W. S., Barnett, L. A. K., deReynier, Y., DiCosimo, J., Fenske, K. H., Gaichas, S. K., Hollowed, A., Holsman, K., Karnauskas, M., Kobayashi, D., Leising, A., Manderson, J. P., McClure, M., Morrison, W. E., … Link, J. S. (2019). Accounting for shifting distributions and changing productivity in the development of scientific advice for fishery management. *ICES Journal of Marine Science*, *76*, 1305–1315. https://doi.org/10.1093/icesjms/fsz048

Keister, J. E., Winans, A. K., & Herrmann, B. (2020). Zooplankton community response to seasonal hypoxia: A test of three hypotheses. *Diversity*, *12*, 21. https://doi.org/10.3390/d12010021

Keller, A. A., Ciannelli, L., Wakefield, W. W., Simon, V., Barth, J. A., & Pierce, S. D. (2017). Species-specific responses of demersal fishes to near-bottom oxygen levels within the California Current large marine ecosystem. *Marine Ecology Progress Series*, *568*, 151–173. https://doi.org/10.3354/meps12066

Klein, E. S., Smith, S. L., & Kritzer, J. P. (2017). Effects of climate change on four New England groundfish species. *Reviews in Fish Biology and Fisheries*, *27*, 317–338. https://doi.org/10.1007/s11160-016-9444-z

Kristensen, K., Nielsen, A., Berg, C. W., Skaug, H., & Bell, B. M. (2016). TMB: Automatic Differentiation and Laplace Approximation. *Journal of Statistical Software*, *70*, 1–21. https://doi.org/10.18637/jss.v070.i05

Kumagai, N. H., Molinos, J. G., Yamano, H., Takao, S., Fujii, M., & Yamanaka, Y. (2018). Ocean currents and herbivory drive macroalgae-to-coral community shift under climate warming. *Proceedings of the National Academy of Sciences*, *115*, 8990–8995. https://doi.org/10.1073/pnas.1716826115

Latimer, A. M., Banerjee, S., Sang, H. Jr, Mosher, E. S., & Silander, J. A. Jr (2009). Hierarchical models facilitate spatial analysis of large data sets: A case study on invasive plant species in the northeastern United States. *Ecology Letters*, *12*, 144–154. https://doi.org/10.1111/j.1461-0248.2008.01270.x

Laurel, B. J., & Rogers, L. A. (2020). Loss of spawning habitat and prerecruits of Pacific cod during a Gulf of Alaska heatwave. *Canadian Journal of Fisheries and Aquatic Sciences*, *77*, 644–650. https://doi.org/10.1139/cjfas-2019-0238

Laurel, B. J., Stoner, A. W., & Hurst, T. P. (2007). Density-dependent habitat selection in marine flatfish: The dynamic role of ontogeny and temperature. *Marine Ecology Progress Series*, *338*, 183–192. https://doi.org/10.3354/meps338183

Lenoir, J., Bertrand, R., Comte, L., Bourgeaud, L., Hattab, T., Murienne, J., & Grenouillet, G. (2020). Species better track climate warming in the oceans than on land. *Nature Ecology and Evolution*, *4*, 1044–1059. https://doi.org/10.1038/s41559-020-1198-2

Levin, L. A., & Le Bris, N. (2015). The deep ocean under climate change. *Science*, *350*, 766–768. https://doi.org/10.1126/science.aad0126

Li, L., Hollowed, A. B., Cokelet, E. D., Barbeaux, S. J., Bond, N. A., Keller, A. A., King, J. R., McClure, M. M., Palsson, W. A., Stabeno, P. J., & Yang, Q. (2019). Subregional differences in groundfish distributional responses to anomalous ocean bottom temperatures in the northeast Pacific. *Global Change Biology*, *25*, 2560–2575. https://doi.org/10.1111/gcb.14676

Lindgren, F., Rue, H., & Lindström, J. (2011). An explicit link between Gaussian fields and Gaussian Markov random fields: The stochastic partial differential equation approach. *Journal of the Royal Statistical Society: Series B (Statistical Methodology)*, *73*(4), 423–498. https://doi.org/10.1111/j.1467-9868.2011.00777.x

Loarie, S. R., Duffy, P. B., Hamilton, H., Asner, G. P., Field, C. B., & Ackerly, D. D. (2009). The velocity of climate change. *Nature*, *462*, 1052–1055. https://doi.org/10.1038/nature08649

Loher, T. (2011). Analysis of match-mismatch between commercial fishing periods and spawning ecology of Pacific halibut (*Hippoglossus Stenolepis*), based on winter surveys and behavioural data from electronic archival tags. *ICES Journal of Marine Science*, *68*, 2240–2251. https://doi.org/10.1093/icesjms/fsr152

Love, M. S. (2011). *Certainly more than you want to know about the fishes of the Pacific Coast: A postmodern experience*. Really Big Press.

MacCall, A. D. (1990). *Dynamic geography of marine fish populations*. Washington Sea Grant Program.

Madeira, C., Mendonça, V., Leal, M. C., Flores, A. A., Cabral, H. N., Diniz, M. S., & Vinagre, C. (2017). Thermal stress, thermal safety margins and acclimation capacity in tropical shallow waters–An experimental approach testing multiple end-points in two common fish. *Ecological Indicators*, *81*, 146–158. https://doi.org/10.1016/j.ecolind.2017.05.050

Massiot-Granier, F., Lassalle, G., Almeida, P. R., Aprahamian, M., Castonguay, M., Drouineau, H., García-Berthou, E., Laffaille, P., Lechêne, A., Lepage, M., Limburg, K., Lobry, J., Rochard, E., Rose, K., Rosebery, J., Rougier, T., Waldman, J., Wilson, K., & Lambert, P. (2018). A generic method to assess species exploratory potential under climate change. *Ecological Indicators*, *90*, 615–623. https://doi.org/10.1016/j.ecolind.2018.03.047

Maureaud, A. A., Frelat, R., Pécuchet, L., Shackell, N., Mérigot, B., Pinsky, M. L., Amador, K., Anderson, S. C., Arkhipkin, A., Auber, A., & Barri, I. (2021). Are we ready to track climate-driven shifts in marine species across international boundaries? A global survey of scientific bottom trawl data. *Global Change Biology*, *27*, 220–236. https://doi.org/10.1111/gcb.15404

Mindel, B. L., Webb, T. J., Neat, F. C., & Blanchard, J. L. (2016). A trait-based metric sheds new light on the nature of the body size–depth relationship in the deep sea. *Journal of Animal Ecology*, *85*, 427–436. https://doi.org/10.1111/1365-2656.12471

Molinos, J. G., Schoeman, D. S., Brown, C. J., & Burrows, M. T. (2019). VoCC: An R package for calculating the velocity of climate change and related climatic metrics. *Methods in Ecology and Evolution*, *10*, 2195–2202. https://doi.org/10.1111/2041-210X.13295

Morley, J. W., Selden, R. L., Latour, R. J., Frölicher, T. L., Seagraves, R. J., & Pinsky, M. L. (2018). Projecting shifts in thermal habitat for 686 species on the North American continental shelf. *PLoS One*, *13*, e0196127. https://doi.org/10.1371/journal.pone.0196127

Nye, J. A., Link, J. S., Hare, J. A., & Overholtz, W. J. (2009). Changing spatial distribution of fish stocks in relation to climate and population size on the Northeast United States continental shelf. *Marine Ecology Progress Series*, *393*, 111–129. https://doi.org/10.3354/meps08220

Oestreich, W. K., Chapman, M. S., & Crowder, L. B. (2020). A comparative analysis of dynamic management in marine and terrestrial systems. *Frontiers in Ecology and the Environment*, *18*, 496–504. https://doi.org/10.1002/fee.2243

Okey, T. A., Alidina, H. M., Lo, V., & Jessen, S. (2014). Effects of climate change on Canada's Pacific marine ecosystems: A summary of scientific knowledge. *Reviews in Fish Biology and Fisheries*, *24*, 519–559. https://doi.org/10.1007/s11160-014-9342-1

Oldfather, M. F., Kling, M. M., Sheth, S. N., Emery, N. C., & Ackerly, D. D. (2020). Range edges in heterogeneous landscapes: Integrating geographic scale and climate complexity into range dynamics. *Global Change Biology*, *26*, 1055–1067. https://doi.org/10.1111/gcb.14897

Ordonez, A., & Williams, J. W. (2013). Projected climate reshuffling based on multivariate climate-availability, climate-analog, and climate-velocity analyses: Implications for community disaggregation. *Climatic Change*, *119*, 659–675. https://doi.org/10.1007/s10584-013-0752-1

Parmesan, C., & Yohe, G. (2003). A globally coherent fingerprint of climate change impacts across natural systems. *Nature*, *421*, 37–42. https://doi.org/10.1038/nature01286

Peña, M. A., Fine, I., & Callendar, W. (2019). Interannual variability in primary production and shelf-offshore transport of nutrients along the northeast Pacific Ocean margin. *Deep Sea Research Part II: Topical Studies in Oceanography*, *169-170*, 169–170. https://doi.org/10.1016/j.dsr2.2019.104637

Perry, A. L., Low, P. J., Ellis, J. R., & Reynolds, J. D. (2005). Climate change and distribution shifts in marine fishes. *Science*, *308*, 1912–1915. https://doi.org/10.1126/science.1111322

Peterson, W., Robert, M., & Bond, N. (2015). The warm blob-conditions in the northeastern Pacific Ocean. *PICES Press*, *23*, 36.

Pinsky, M. L., & Fogarty, M. (2012). Lagged social-ecological responses to climate and range shifts in fisheries. *Climatic Change*, *115*, 883–891. https://doi.org/10.1007/s10584-012-0599-x

Pinsky, M. L., Rogers, L. A., Morley, J. W., & Frölicher, T. L. (2020). Ocean planning for species on the move provides substantial benefits and requires few trade-offs. *Science Advances*, *6*, eabb8428. https://doi.org/10.1126/sciadv.abb8428

Pinsky, M. L., Worm, B., Fogarty, M. J., Sarmiento, J. L., & Levin, S. A. (2013). Marine taxa track local climate velocities. *Science*, *341*, 1239–1242. https://doi.org/10.1126/science.1239352

Plagányi, É. E., Weeks, S. J., Skewes, T. D., Gibbs, M. T. et al (2011). Assessing the adequacy of current fisheries management under changing climate: A southern synopsis. *ICES Journal of Marine Science*, *68*, 1305–1317. https://doi.org/10.1093/icesjms/fsr049

Pörtner, H., Bock, C., Knust, R., Lannig, G., Lucassen, M., Mark, F., & Sartoris, F. (2008). Cod and climate in a latitudinal cline: Physiological analyses of climate effects in marine fishes. *Climate Research*, *37*, 253–270. https://doi.org/10.3354/cr00766

Pörtner, H. O., Roberts, D. C., Masson-Delmotte, V., Zhai, P., Tignor, M., Poloczanska, E., Mintenbeck, K., Nicolai, M., Okem, A., Petzold, J., Rama, B., & Weyer, N. (2019). *IPCC special report on the ocean and cryosphere in a changing climate*. Cambridge University Press.

Punt, A. E., A'mar, T., Bond, N. A., Butterworth, D. S., de Moor, C. L., De Oliveira, J. A. A., Haltuch, M. A., Hollowed, A. B., & Szuwalski, C. (2014). Fisheries management under climate and environmental uncertainty: Control rules and performance simulation. *ICES Journal of Marine Science*, *71*, 2208–2220. https://doi.org/10.1093/icesjms/fst057

R Core Team. (2019). *R: A Language and Environment for Statistical Computing*. R Foundation for Statistical Computing.

Rindorf, A., & Lewy, P. (2006). Warm, windy winters drive cod north and homing of spawners keeps them there. *Journal of Applied Ecology*, *43*, 445–453. https://doi.org/10.1111/j.1365-2664.2006.01161.x

Rooper, C. N., Ortiz, I., Hermann, A. J., Laman, N., Cheng, W., Kearney, K., & Aydin, K. (2020). Predicted shifts of groundfish distribution in the Eastern Bering Sea under climate change, with implications for fish populations and fisheries management. *ICES Journal of Marine Science*, *78*(1), 220–234. https://doi.org/10.1093/icesjms/fsaa215

Rue, H., Martino, S., & Chopin, N. (2009). Approximate Bayesian inference for latent Gaussian models by using integrated nested Laplace approximations. *Journal of the Royal Statistical Society: Series B (Statistical Methodology)*, *71*, 319–392. https://doi.org/10.1111/j.1467-9868.2008.00700.x

Serra-Diaz, J. M., Franklin, J., Ninyerola, M., Davis, F. W., Syphard, A. D., Regan, H. M., & Ikegami, M. (2014). Bioclimatic velocity: The pace of species exposure to climate change. *Diversity and Distributions*, *20*, 169–180. https://doi.org/10.1111/ddi.12131

Shackell, N. L., Frank, K. T., Fisher, J. A. D., Petrie, B., & Leggett, W. C. (2010). Decline in top predator body size and changing climate alter trophic structure in an oceanic ecosystem. *Proceedings of the Royal Society B: Biological Sciences*, *277*, 1353–1360. https://doi.org/10.1098/rspb.2009.1020

Shelton, A. O., Thorson, J. T., Ward, E. J., & Feist, B. E. (2014). Spatial semiparametric models improve estimates of species abundance and distribution. *Canadian Journal of Fisheries and Aquatic Sciences*, *71*, 1655–1666. https://doi.org/10.1139/cjfas-2013-0508

Sinclair, A., Schnute, J., Haigh, R., Starr, P., Stanley, R., Fargo, J., & Workman, G. (2003). Feasibility of multispecies groundfish bottom trawl surveys on the BC coast. DFO Canadian Science Advisory Secretariat (CSAS) Research Document 2003/049.

Stock, C. A., Alexander, M. A., Bond, N. A., Brander, K. M., Cheung, W. W. L., Curchitser, E. N., Delworth, T. L., Dunne, J. P., Griffies, S. M., Haltuch, M. A., Hare, J. A., Hollowed, A. B., Lehodey, P., Levin, S. A., Link, J. S., Rose, K. A., Rykaczewski, R. R., Sarmiento, J. L., Stouffer, R. J., … Werner, F. E. (2011). On the use of IPCC-class models to assess the impact of climate on living marine resources. *Progress in Oceanography*, *88*, 1–27. https://doi.org/10.1016/j.pocean.2010.09.001

Sunday, J. M., Pecl, G. T., Frusher, S., Hobday, A. J., Hill, N., Holbrook, N. J., Edgar, G. J., Stuart-Smith, R., Barrett, N., Wernberg, T., Watson, R. A., Smale, D. A., Fulton, E. A., Slawinski, D., Feng, M., Radford, B. T., Thompson, P. A., & Bates, A. E. (2015). Species traits and climate velocity explain geographic range shifts in an ocean-warming hotspot. *Ecology Letters*, *18*, 944–9530. https://doi.org/10.1111/ele.12474

Szuwalski, C. S., & Hollowed, A. B. (2016). Climate change and non-stationary population processes in fisheries management. *ICES Journal of Marine Science*, *73*, 1297–1305. https://doi.org/10.1093/icesjms/fsv229

Thorson, J. T., & Barnett, L. A. K. (2017). Comparing estimates of abundance trends and distribution shifts using single- and multispecies models of fishes and biogenic habitat. *ICES Journal of Marine Science*, *74*, 1311–1321. https://doi.org/10.1093/icesjms/fsw193

Thorson, J. T., Fonner, R., Haltuch, M. A., Ono, K., & Winker, H. (2017). Accounting for spatiotemporal variation and fisher targeting when estimating abundance from multispecies fishery data. *Canadian Journal of Fisheries and Aquatic Sciences*, *74*, 1794–1807. https://doi.org/10.1139/cjfas-2015-0598

Thorson, J. T., Pinsky, M. L., & Ward, E. J. (2016). Model-based inference for estimating shifts in species distribution, area occupied and centre of gravity. *Methods in Ecology and Evolution*, *7*, 990–1002. https://doi.org/10.1111/2041-210X.12567

Thorson, J. T., Rindorf, A., Gao, J., Hanselman, D. H., & Winker, H. (2016). Density-dependent changes in effective area occupied for sea-bottom-associated marine fishes. *Proceedings of the Royal Society B: Biological Sciences*, *283*, 20161853. https://doi.org/10.1098/rspb.2016.1853

Thorson, J. T., Scheuerell, M. D., Shelton, A. O., See, K. E., Skaug, H. J., & Kristensen, K. (2015) Spatial factor analysis: A new tool for estimating joint species distributions and correlations in species range. *Methods in Ecology and Evolution 6*, 627--637. https://doi.org/10.1111/2041-210X.12359

Thorson, J. T., Shelton, A. O., Ward, E. J., & Skaug, H. J. (2015). Geostatistical delta-generalized linear mixed models improve precision for estimated abundance indices for West Coast groundfishes. *ICES Journal of Marine Science*, *72*, 1297–1310. https://doi.org/10.1093/icesjms/fsu243

Tommasi, D., Stock, C. A., Hobday, A. J., Methot, R., Kaplan, I. C., Eveson, J. P., Holsman, K., Miller, T. J., Gaichas, S., Gehlen, M., Pershing, A., Vecchi, G. A., Msadek, R., Delworth, T., Eakin, C. M., Haltuch, M. A., Séférian, R., Spillman, C. M., Hartog, J. R., … Werner, F. E. (2017). Managing living marine resources in a dynamic environment: The role of seasonal to decadal climate forecasts. *Progress in Oceanography*, *152*, 15–49. https://doi.org/10.1016/j.pocean.2016.12.011

Turris, B. R. (2000). A comparison of British Columbia's ITQ fisheries for groundfish trawl and sablefish: Similar results from programmes with differing objectives, designs and processes. *FAO Fisheries Technical Paper*, 254–261.

Tweedie, M. C. K. (1984). An index which distinguishes between some important exponential families. In J. K. Gosh, & J. Roy (Eds.), *Statistics: Applications and new directions. Proceedings of the Indian statistical institute golden jubilee international conference* (pp. 579–604). Indian Statistical Institute Calcutta.

VanDerWal, J., Murphy, H. T., Kutt, A. S., Perkins, G. C., Bateman, B. L., Perry, J. J., & Reside, A. E. (2013). Focus on poleward shifts in species' distribution underestimates the fingerprint of climate change. *Nature Climate Change*, *3*, 239–243. https://doi.org/10.1038/nclimate1688

Wallace, S., Turris, B., Driscoll, J., Bodtker, K., Mose, B., & Munro, G. (2015). Canada's Pacific groundfish trawl habitat agreement: A global first in an ecosystem approach to bottom trawl impacts. *Marine Policy*, *60*, 240–248. https://doi.org/10.1016/j.marpol.2015.06.028

Ward, E. J., Jannot, J. E., Lee, Y. W., Ono, K., Shelton, A. O., & Thorson, J. T. (2015). Using spatiotemporal species distribution models to identify temporally evolving hotspots of species co-occurrence. *Ecological Applications*, *25*, 2198–2209. https://doi.org/10.1890/15-0051.1

Webster, R. A., Soderlund, E., Dykstra, C. L., & Stewart, I. J. (2020). Monitoring change in a dynamic environment: Spatiotemporal modelling of calibrated data from different types of fisheries surveys of pacific halibut. *Canadian Journal of Fisheries and Aquatic Sciences*, *77*, 1421–1432. https://doi.org/10.1139/cjfas-2019-0240

Williams, D. C., Nottingham, M. K., Olsen, N., & Wyeth, M. R. (2018). Summary of the Queen Charlotte Sound synoptic bottom trawl survey, July 6 – August 8, 2015. *DFO Canadian Manuscript Report of Fisheries and Aquatic Sciences*. *3136*, viii + 64 p.

SUPPORTING INFORMATION

Additional supporting information may be found in the online version of the article at the publisher's website.

How to cite this article: English, P. A., Ward, E. J., Rooper, C. N., Forrest, R. E., Rogers, L. A., Hunter, K. L., Edwards, A. M., Connors, B. M., & Anderson, S. C. (2022). Contrasting climate velocity impacts in warm and cool locations show that effects of marine warming are worse in already warmer temperate waters. *Fish and Fisheries*, 23, 239–255. https://doi.org/10.1111/faf.12613